THE PERFORMANCE OF FIBER REINFORCEMENT IN COMPLETELY DECOMPOSED GRANITE

B.N. Madhusudhan[1*], B.A. Baudet[2], P.M.V. Ferreira[3] and P. Sammonds[4]

[1*]Research Fellow, University of Southampton, UK, SO17 1BJ; mbnm1f13@soton.ac.uk; formerly, Post-doctoral Researcher, The University of Hong Kong, Hong Kong

[2]Lecturer, University College London, UK, WC1E 6BT; formerly, Assistant Professor, The University of Hong Kong, Hong Kong

[3] Lecturer, University College London, UK, WC1E 6BT;

[4]Professor of Geophysics, University College London, UK, WC1E 6BT;

Abstract

Adding discrete fibers to soils can improve their strength, however fiber reinforcement remains scarce in practice. Previous studies on the performance of soils reinforced with discrete fibers consist mainly of laboratory studies with either clay or, most often, uniform sand as the host soil, so that there is a lack of data on other types of soils such as weathered soils, which tend to be well graded. Unlike uniform soils, which are generally dilative, well graded soils usually show a contractive behavior. This study examines the effect of adding fibers to a completely decomposed granite (CDG) typical of many residual soils which has the characteristics to be sensitive to material and sample preparation and also to be compressive during shearing. It is found that adding discrete fibers to the CDG homogenizes it as the reinforced soil is not sensitive to the method of material or sample preparation. It is also found that despite its compressive nature, fibers mobilize extra strength compared to the unreinforced soil, and this effect does not reduce at large confining stresses.

Keywords: residual soils; reinforced soils; laboratory tests

Introduction

The large body of work on the potential use of fibers to improve the performance of soils consists mainly of laboratory tests or constitutive modelling (e.g. Maher and Gray, 1990; Maher and Ho, 1994; Michalowski and Cermak, 2003; Silva dos Santos et al., 2010; Ajayi et al., 2015; Diambra and Ibraim, 2015), and seldom in-situ application (e.g. Gregory, 2011). Including discrete fibers to a soil has proved to have a favorable effect on the soil's mechanical properties (e.g. Consoli et al., 2005; Gray and Ohashi, 1983; Maher and Gray, 1990; Silva dos Santos et al., 2010 and references that follow). The performance of fiber-reinforced soils is dependent on establishing an optimum dosage of the fibers for the given soil. The increase in strength is generally proportional to the quantity of reinforcement, but a limiting content is usually reached when an optimum number of fibers that participate actively in the fiber-soil mixture behavior is reached (Gray and Al-Rafeai, 1986). Beyond that limiting content there is no significant increase in strength. Zornberg (2005) found that in both clay and sand, adding fibers between 25 mm and 50 mm, in percentages of 0 to 0.4% by weight, contributes to increasing the peak strength. Optimizing a fiber type and quantity is difficult, and he found that at low fiber contents, fibers with a higher aspect ratio could provide the same performance as fibers with a lower aspect ratio.

Using uniform sand as host soil (e.g. Consoli et al., 2005; Silva dos Santos et al., 2010; Diambra et al., 2013) offers the advantage that it is simple to characterize (single mineralogy, uniform size), with a well-defined behavior in compression and shearing so that patterns of behavior associated solely with fiber reinforcement can be more easily identified. Some studies were performed on sands with various gradations (e.g. Maher and Gray, 1990), or clay (e.g. Maher and Ho, 1994; Ghazavi and Roustaie, 2010), highlighting the effect of the soil particle size distribution, particle shape and cohesion on the fiber reinforcement. Some researchers did study the performance of discrete fibers added to their local soil, for example Consoli et al.

(2003) or Heineck et al. (2005) used a residual sandstone from Brazil as the host soil, but its non-convergent behavior (refer to Ferreira and Bica, 2006) hindered any characterization within a recognized framework such as the Critical State framework, and therefore made it difficult to distinguish clearly the effects of the fibers alone. Later on, the same researchers switched to using a uniform sand that would allow studying the fundamental behavior of the reinforced soil within the Critical State framework (e.g. Consoli et al., 2005). The behavior of uniform sand reinforced with discrete fibers is now better established but it is unclear whether the framework determined, for example, by Silva dos Santos et al. (2010), applies to other types of soils such as weathered soils, well graded soils or larger-scale railway ballast (e.g. Ajayi et al., 2015). This study used completely decomposed granite from Hong Kong (CDG) as host soil, a weathered soil which has the characteristics to be sensitive to material and sample preparation and also to be compressive during shearing. It will be shown, using compression and shearing test data analyzed within the Critical State framework, that adding discrete fibers to the CDG homogenizes it as the reinforced soil is not sensitive to the method of material or sample preparation. It will also be shown that despite the compressive nature of the CDG, fibers mobilize extra strength compared to the unreinforced soil, and this effect does not reduce at large confining stresses.

The host soil used here is similar to many residual soils encountered in Europe (Viana da Fonseca et al., 2006), Asia (Lee and Coop, 1995) and America (Ferreira and Bica, 2006). The main characteristic is the well-graded particle size distribution with a non-negligible fines content. Unlike uniform sands, which are dilative at low to medium pressures, well-graded CDG displays contractive behavior from low stress levels. Given that fibers are thought to work predominantly in tension (e.g. Consoli et al., 2005; Diambra and Ibraim, 2015), using them in a compressive soil will bring more insight about their mechanics of reinforcement. Particular to the host soil chosen, is how the effect of sample preparation, which is pronounced in the unreinforced CDG (Madhusudhan and Baudet, 2014), affects the reinforcement. Like in many studies on granular soils (e.g. Coop and Lee, 1993; Altuhafi et al., 2010; Silva dos Santos et al., 2010), the data presented extend beyond the applicable engineering stress range so that recognizable features of critical state soil mechanics, such as normal compression and critical state lines, could be identified to provide a platform for comparison with other unreinforced and reinforced soils and future modelling.

Materials, procedures and testing apparatus

Oedometer and triaxial tests were performed on specimens of completely decomposed granite from Hong Kong with and without fiber reinforcement. The material used and the different methods of preparation adopted are described below.

Materials

The completely decomposed granite (CDG) was obtained at Mt. Beacon, Kowloon Tong, Hong Kong. It is a well-graded soil, with about 20% fines and a plasticity index of 16%. The mineralogy of the soil, analyzed through EDX measurements, consists of potassium feldspar, quartz and mica, with some kaolinite present in the clay fraction. In its natural disturbed state, the soil consists of weakly bonded clusters of particles ranging from coarse sand to clay which can be easily broken down. The maximum dry density determined by Proctor compaction is 18.91 kN/m^3 for an optimum water content of 11%.

Polypropylene fibers, similar to those used by Silva dos Santos et al. (2010), were utilized to enable comparisons with the performance of a uniform sand reinforced with the same type of fibers. These fibers are chemically inert and have uniform characteristics, with a specific gravity of 0.91, a tensile resistance of 120 MPa, an elastic modulus of 3 GPa and a range of linear deformation at rupture between 80% and 170%. The fibers, 0.023 mm diameter, are manufactured as clusters and, before each test, the required amount of fibers was immersed in a water-filled container where a slow-speed egg blender was activated for about 10 minutes, ensuring the separation of the fibers. Two fiber lengths, 24 mm and 50mm, and two fiber contents, 0.1% and 0.3% by weight, were selected. Previous studies used fibers lengths between 24 and 50 mm and up to 0.9 % fibers by weight, with many studies using 0.5% by weight of 24 mm fibers (e.g. Heineck et al., 2005; Silva dos Santos et al., 2010; Diambra et al., 2013). Preliminary work with the CDG showed that dosages higher than 0.3% made it difficult to create homogeneously reinforced specimens as the fibers occupied too much of the specimen volume.

Material preparation:

The soil collected was prepared according to the specifications below:

Hand Destructuration (**D**): The soil samples collected were destructured by hand until all particles passed through a 5mm sieve.

Fines reconstitution (**F**): The fines were separated from the hand destructured CDG by wet sieving through a 63 μm sieve. Once the soil and the fines removed were air-dried, they were mixed together in the original proportions.

Sample preparation:

Moist-tamped (**M**): The soil and the separated wet fibers were thoroughly mixed by hand at the optimum water content of 11 %, until a homogeneous mixture was achieved. The mixture was placed directly onto the triaxial pedestal using the under-compaction method proposed by Ladd (1978) to create loose specimens. Dense specimens were prepared by tamping the soil carefully using a 76 mm diameter compaction mold. The specimen was later flushed with de-aired water and allowed to dry in the oven for 24 hours at 50^{o}C. Both the loose and dense samples were moist-tamped in five layers to achieve the target density (Ladd, 1978). Because of the significant volume changes that typically occurred before saturation, due to macro-voids, the initial dimensions were recorded after saturation by CO2 and de-aired water flushing while maintaining a small suction (<20kPa) (Madhusudhan & Baudet, 2014; Yan & Li, 2012). This method was applied to both soil prepared by hand destructuration and soil prepared by fines reconstitution (which will be referred to in the test identification as MD and MF respectively, see detail later).

Slurry (**S**): The soil and fibers were well mixed at a water content close to the liquid limit. For loose specimens, the slurry was deposited directly into a mold on the triaxial pedestal. A small suction was applied overnight using a burette placed 1m below the pedestal. For dense specimens, dead weights were placed on the soil inside of the mold to reach a target density. This normally took around six hours. This method was applied to the hand destructured soil (noted as SD in the test identification, see detail later).

Dry Deposition (**D**): Hand destructured soil was sieved through 5mm sieve and deposited using a hopper of 20 mm neck at zero falling height into the mould to prepare loose specimens. For medium dense specimens, the soil was dry deposited and lightly tamped into appropriate split mould. It was then flushed with distilled water and oven-dried for 24 h at 500C, in order to eliminate macro-voids without the problem of segregation. The oven dried cylindrical specimens were then transferred to the triaxial pedestal and saturated by carbon dioxide (CO2) followed by de-aired water circulation under a suction of 20 kPa. Those specimens are referred in the test identification as DD (see detail later).

Testing procedures and apparatus

The testing program was designed so as to emphasize the effect of the material preparation, the fiber type and dosage and the added performance when compared to the unreinforced soil. The first series of tests consisted of triaxial tests on 76 mm diameter specimens to compare the effects of fiber length and fiber quantity: type A – fiber length of 24mm and fiber content of 0.3%; type C – fiber length of 50mm and fiber content of 0.3%; type D – fiber length of 50mm and fiber content of 0.1% (Table 1). Ang and Loehr (2003) showed that 70 mm specimens used with 50 mm fibers (i.e. a ratio of 1.4 between specimen size and fiber length) were representative of the larger reinforced soil mass. Once the optimum fiber mixture of 24 mm and 0.3% was determined, compression was investigated primarily via oedometer tests, whilst shearing was investigated via standard (76 mm diameter) and high pressure (38 mm diameter) triaxial tests. For these tests on smaller specimens, the ratio between specimen diameter and fiber length is about 1.5, which is typical in studies on fiber-soil mixtures (e.g. Silva dos Santos et al., 2010; Diambra et al., 2013), and is also consistent with the ratio of 1.4 used by Ang and Loehr (2003).

In Table 1, the test identification is given in the first column, which contains details about the material and sample preparation: reinforced (R)/unreinforced (U), the type of fiber combination (A, C or D), sample number (1 or 2), sample preparation (M, S or D), material preparation (D or F) and the effective stress at which the sample was sheared. Samples MD, i.e. hand destructured and moist tamped, were thought to represent best the in-situ compaction, whilst samples prepared using SD (i.e. hand destructured and made into a slurry) and MF (i.e. made by fines reconstitution and moist-tamping) are believed to represent better the extreme weather conditions during the rainy season, when the fines may become separated from the coarse soil grains.

<u>Triaxial testing</u>: Undrained and drained compression tests were carried out on specimens of 76 mm diameter and 152 mm height, using a standard triaxial apparatus mounted on an automated loading frame. Normally consolidated specimens were tested under effective confining stresses of 50, 100 kPa, 200kPa and 500 kPa while a few over-consolidated specimens were tested

under confining stresses of 50, 100 and 200 kPa. The cell pressure and back pressure (applied at the bottom of the specimen) were monitored with GDS controllers of 2 MPa capacity, and the axial strains were measured by an external displacement transducer. The shear strain was calculated as $\varepsilon_s = \varepsilon_a - 1/3\ \varepsilon_v$, with ε_a and ε_v being the axial and volumetric strains. The pore water pressure was measured at the top of the specimens. Precautions were taken to reduce the friction between the end platens and specimen by using smaller porous stones flush with the platens. Each specimen was covered by two latex membranes smeared with room temperature vulcanizing silicon rubber coating wherever sharp edges were felt. Appropriate membrane corrections were applied (Head, 1980). The specific volume was obtained by four expressions using independent variables such as the initial and final weights and volumes of the soil specimen, following the method described in Madhusudhan and Baudet (2014). The difference between the maximum and minimum initial specific volumes, calculated in this way, is reported in Table 1 as specific volume precision. The average precision was 0.023 for both the reinforced specimens and the unreinforced CDG. The fibers were considered as solids in the calculations. The specific gravity of the fiber-CDG mixture was taken equal to that of the unreinforced CDG, which was determined in laboratory to be 2.65, as it was found that the effect of adding 0.3% fibers or less by weight had a negligible influence on the specific gravity (less than 1%) and on the specific volume (less than 0.02). The summary of the tests and accuracy of the specific volumes are given in Table 1, where v_0 refers to the initial specific volume, v_c refers to the specific volume before shearing and HP identifies the triaxial tests that were carried out at high pressures.

Complementary high pressure triaxial compression tests were carried out on specimens prepared with 24 mm fibers, at University College London, using an apparatus described in Altuhafi et al. (2010), capable of reaching pressures up to 20 MPa. The specimens tested had 38 mm diameter by 76 mm height and were prepared using the moist-tamping and slurring methods. For these tests, the puncture of the membrane was avoided by using two neoprene membranes. Details about these tests are also presented in Table 1.

Oedometer testing: Some specimens prepared with 24 mm fibers were tested in one-dimensional compression using a floating ring oedometer cell of 38mm diameter and 25mm height. The specimens were created directly into the oedometer cell after smearing its inner surface with a thin layer of silicon grease. They were then saturated in a water bath for 12-15 hours before compression to 15 MPa for the moist-tamped specimens and 24 MPa for the slurried ones. The initial specific volume was calculated by four different methods that made use of the initial height of the specimen, measured by calliper and by dial gauge (resolution 0.01 mm), and the final height (see Madhusudhan and Baudet, 2014). The results presented are for tests in which the void ratios calculated with the four methods fall within a range of ±0.01.

Selection of fiber-CDG mixture

A comparison of the performance of the three fiber combinations (A, C and D) in shearing is shown in Figure 1, using data from reinforced and unreinforced specimens sheared from similar void ratios for a given confining stress (Table 1). Plain lines are used for the reinforced specimens and dashed lines for the unreinforced ones. The sample preparation methods are differentiated by using open symbols for moist-tamping and closed symbols for fines reconstitution or slurry, although it will be shown later that the sample preparation does not affect the results of the reinforced specimens in the same way as it does for the unreinforced soil. A first observation is that the specimens with a fiber content of 0.1% (type D; specimens RD1MD100 and RD1MF500) show no improvement on the strength for any material or sample preparation method. The specimens prepared with 0.3% of 24 mm fibers (type A) show the best performance, with the strength multiplied by about 2.3 at low pressure (RA1MD100). Specimen RA1SD500 reaches a lower stress ratio but it will be shown later that it is not due to the higher confining stress but is more likely to be test specific. Using longer fibers of 50 mm (RC1SD100) does not add any benefit to the reinforced soil strength. The method of preparation does not seem to affect the strength, the curves for specimens RA1MD100 and RC1SD100 plotting close to each other. The performance of the fibers is particularly significant after 10% shear strain, where additional strength is gained until a critical state is reached.

Based on the stress dilatancy graph shown in Figure 1b, it is observed that the inclusion of fibers makes the volumetric response more contractive during tests at low confining stress (when compared to the unreinforced specimen URSD100), whilst no significant change is noticed for higher stress levels. The unreinforced (URDD500) and reinforced specimens follow the same stress dilatancy path at the start of the tests, showing that the current strength is mobilized as compressive volumetric strains develop. The unreinforced specimens reach critical state at a stress ratio M = 1.57. The paths of the fiber-CDG mixtures become steeper from about $d\varepsilon_v/d\varepsilon_s=0.2$ as the fiber reinforcement becomes effective at large deformation, possibly owing to lock-in of the fibers between grains as the particles re-arrange. As observed in the stress-strain curves, the type-D fiber combination, which only contains 0.1% fiber, leads to the lower strength with a stress ratio M at critical state of 1.83, while the specimens with a higher fiber content of 0.3% reach values M = 2.25 for 24 mm fibers (type A) and M = 1.83 for 50 mm fibers (type C). The steepening of the stress dilatancy path towards critical state concurs with the late increase in strength observed in Figure 1a, at about 10% shear strain, which also marks the beginning of different stiffnesses. Based on these results, the research then focused on investigating the behavior of type-A mixtures (i.e. with 0.3% of 24 mm fibers) and comparing it with that of the unreinforced soil.

Compression behavior

The location of the normal compression line (NCL) of the unreinforced CDG is sensitive to the method of material and sample preparation, with the NCL of specimens prepared by fines reconstitution or by hand destructuration and slurry lying above that of specimens prepared by hand destructuration and moist-tamping (Madhusudhan and Baudet, 2014). The influence of the material and sample preparation method is evident in both one-dimensional and isotropic normal compression lines (Fig. 2). Figure 2a shows the compression data obtained from oedometer tests; the curves for the unreinforced specimens prepared by fines reconstitution or by hand destructuration and slurry (open circles) converge to a line distinctly separate from the curve reached by the unreinforced specimens prepared by hand destructuration and moist-tamping or dry deposition (open diamonds). Washing the CDG or using a large amount of water in the sample preparation displaces the particles, creating fabrics that can reach higher values of mean effective stress. In contrast, the curves for the fiber-reinforced specimens, which were all prepared by hand destructuration and are represented by closed symbols, converge to a unique normal compression line irrespective of whether the samples were made by moist-tamping or by the slurry method.

Additional K_0-compression and high pressure isotropic compression tests, performed in the triaxial apparatus, show the same pattern (Figure 2b). The reinforced CDG does not seem to be affected by the method of preparation, as if the fibers acted as a homogenizer for the soil. A positive reinforcing effect with a higher strength at a given void ratio is observed when compared to the unreinforced MD specimens, with the isotropic normal compression line (iso-NCL) of the reinforced specimens plotting parallel and above that of the reconstituted specimens. No such improvement is observed when comparing with the unreinforced specimens prepared by fines reconstitution or by slurry (MF or SD). It has been suggested from test results on moist-tamped samples that fibers assist the agglomerates in resisting the compressibility by lock-in of the fibers between sand grains (Consoli et al., 2005). In the reinforced specimens prepared by fines reconstitution or hand destructuration and slurry, the larger amount of fine particles free to move in the specimens does not seem to influence the location and slope of the NCL, suggesting that there may be an overriding effect of the fiber lock-in between coarse particles, creating a unique compression curve for the fiber-soil mixture whatever the method of material or sample preparation.

The compression parameters determined for the fiber-CDG mixture are summarized in Table 2. The parameters for the normal compression lines of the unreinforced CDG, also given in Table 2, were determined by Madhusudhan and Baudet (2014). For moist-tamped specimens, the effect of adding fibers is similar to what was found by Silva dos Santos et al. (2010) on quarzitic sand.

Shearing behavior

Normally and over-consolidated specimens of reinforced CDG were sheared drained or undrained in the triaxial apparatus, most specimens being 76 mm diameter while the high pressure tests were carried out on 38 mm diameter specimens. Typical stress-strain-volume responses are presented in Figure 3, in terms of stress ratio (Fig. 3a) and stress dilatancy (Fig. 3b). As in Figure 1, the curves for the reinforced specimens are represented by plain lines while for unreinforced specimens dashed lines are used, material and sample preparation methods are differentiated by using open symbols for hand destructuration and moist-tamping; closed symbols are used for fines reconstitution or hand destructuration and slurry.

The unreinforced specimens almost all reach a stable stress ratio of 1.57 at large strains (Fig. 3a). The reinforced specimens reach a much higher stress ratio, including those tested under very high confining pressures (RA MD HP and RA SD HP), which were stopped at strains around 15% because of the displacement capacity of the apparatus, at which strain level the stress ratio and volumetric deformations had stabilized or were showing signs to stabilize. This suggests that there is no loss of efficiency of the fibers with increasing stress, unlike what was found in other soils (e.g. Maher and Gray, 1990; Silva dos Santos et al., 2010). Particular to the CDG, this seems to apply whatever the method of preparation (moist tamping or slurry). Two specimens did reach lower stress ratios (RA1MD 200 and RA1SD 500) but given that they were prepared with different methods (MD and SD) and tested at medium pressures, this cannot easily be attributed to either the sample preparation method or the confining stress and is more likely to be an unusual feature of these two tests.

The stress dilatancy plotted in Figure 3b sheds more light on the development of the strength. As noted above, all the unreinforced specimens reach critical state at a stress ratio M = 1.57. The reinforced specimens reach critical state at higher stress ratios generally greater than M = 1.90, and their path becomes steeper from about $\delta\varepsilon_v/\delta\varepsilon_s$=0.2. The data for the high pressure tests are a bit more scattered but they seem to follow the same tendency. There is however a difference with the behavior of reinforced uniform quartzitic sand such as that tested by Silva dos Santos et al. (2010), for which an upwards "tail" in the stress dilatancy is seen, which indicates a very rapid increase in strength with dilation.

Another difference with uniform quartzitic sands, which require strains much larger than those typically reached in triaxial tests to reach a true critical state (e.g. Coop et al., 2004; Muir Wood, 2006), is that while they only reach the steep, linear part of the NCL and CSL (defined as $v = N - \lambda \ln p'$ and $v = \Gamma - \lambda \ln p'$ respectively) at very high stresses, when particle breakage is occurring, well-graded residual soils such as CDG can reach their NCL and true critical state at lower stresses and strains, as seen in Figures 1 and 3. This was also reported by Santucci et al. (1998) and Ferreira and Bica (2006) for silty sand and residual soil. Here critical state was identified as the point at which the stress ratio (q/p') and/or volumetric strain becomes constant, which in most tests - except the high pressure tests - occurred at strains larger than 30% (Figure 3a).

The critical state line for the unreinforced CDG was determined from the stress dilatancy plot in Figure 3b to have a gradient M = 1.57. Madhusudhan and Baudet (2014) found that it is unique and not influenced by the method of preparation. The performance of the fiber-reinforced soil can be assessed by comparing the strength of the reinforced specimens with the critical state strength of the corresponding unreinforced CDG specimens. The end-of-test points, most of them at critical state, are reported in Figure 4a (low stress levels) and Figure 4b (high stress levels). At low stress levels, the data points for the reinforced specimens plot above the critical state line for the unreinforced CDG, forming an almost straight line of slope M = 1.90, which corresponds to the lower bound value found from the stress dilatancy data in Figure 3b. When the critical state lines are extended to high pressures (Figure 4b), the effect of the fiber reinforcement in providing additional strength to the host soil remains even at deviatoric stress levels greater than 100MPa.

Maher and Gray (1990), who tested well graded sands as well as uniform sands, suggested a bilinear failure envelope, with a critical pressure delimiting the pressure range when the fibers may be slipping (low confining stresses) and when they may be resisting pull-out by stretching (high confining stresses), the latter resulting in a failure envelope above and parallel to that of the unreinforced soil. They tested soils up to 500 kPa confining stress and found that well graded sands had a lower critical pressure than uniform sands, and a higher contribution to the strength from the fibers. Their model suggests that the fibers contribute less to the resistance as confining stress levels increase. Silva dos Santos et al. (2010), who performed high pressure tests similarly to this study, had found for a reinforced uniform quarzitic sand that the critical state line is curved, and tends to converge to that of the unreinforced sand at large stresses. Diambra and Ibraim (2015) also found, from analytical studies, that larger tensile stresses are mobilized in fibers as the soil becomes stiffer at large confining stresses. Here, the fibers tested at high confining stress contribute the same amount of strength as those tested at lower pressures (Fig. 3a), about 20%, which is of the order of 20 MPa for the high pressure tests. With an elastic modulus of 3 GPa, this would cause only a small amount of deformation in the fibers. Visual inspection of the fibers after a high pressure test showed that a significant but not extensive number of fibers had broken, and this may also have happened during isotropic compression (Silva dos Santos et al., 2010), although fiber breakage in uniform soil is also caused by nipping, which is less likely in well graded soils. It may also be that the very large stiffness of the fibers compared to that of the CDG allows the large stresses to be taken, while in stiffer soils like quarzitic sands the fibers reach their maximum elongation more rapidly.

The K_0 triaxial compression stress paths of the reinforced and the unreinforced CDG, plotted in Figure 4a, show clearly that each unreinforced sample preparation method has a different value of earth pressure at rest, $K_0 = 0.40$ for the slurried specimen and $K_0 = 0.46$ for the specimen prepared by dry deposition. This may have been caused by the removal of the fines coating of the coarse grains during washing or preparation by slurry, rendering the soil grains rougher and possibly affecting the friction angle. The addition of fibers cancels this effect, the K_0 stress paths of the reinforced specimens tested with different preparation methods are the same, regardless of the method of preparation, and almost coincident with that of the slurried unreinforced specimen, as shown in Figure 4a.

The state paths for all the tests on reinforced specimens tested at low to medium pressures are shown in a plot of specific volume, v, against the logarithm of the mean effective stress, lnp', in Figure 5. When the volumetric response did not reach a stable state, which occurred sometimes in the reinforced soil, when the stress exceeded the load cell capacity, if there was not enough length for the piston to be able to complete the test, or when the tests were stopped at the onset of the shear plane development, the test end points and the direction of the state paths were noted and they are reported with arrows. A unique critical state line can be defined for the fiber-reinforced CDG regardless of the preparation method involved (refer to Table 1). The end-of-test points of the reinforced specimens, found mostly to be at critical state, are replotted in Figure 6 without the state paths for clarity. The high pressure data points, also plotted in Figure 6, are not aligned with the log-line part of the CSL and seem to indicate a much shallower slope. This may be because at those high stresses very low void ratios (close to zero) are reached, since negative void ratios are not possible, the void ratios at critical state may tend to converge to a low value.

While two distinct CSLs were found for the unreinforced soil, which depend on the preparation method (Madhusudhan and Baudet, 2014), a unique CSL can be identified for the reinforced CDG, parallel to the CSLs of the unreinforced soil. As was found earlier for the compression behavior, the addition of fibers seems to act as homogenizer and to cancel the effect of the preparation method in the volumetric response. Ekinci and Ferreira (2012) also found that adding fibers to clay changes the mode of failure by inhibiting the formation of a shear plane. As pointed out earlier, the critical state and normal compression lines do not seem to curve at lower pressures for either unreinforced or reinforced soil (Fig. 6), and the distance between the CSL and NCL appears to be similar for both unreinforced and reinforced specimens. The slopes and intercepts of the critical state lines are reported in Table 2, using, for the unreinforced CDG, the values that were determined by Madhusudhan and Baudet (2014). Similarly to what was found for the NCL, the CSL of the reinforced soil coincides with that of the unreinforced specimens prepared by moist tamping and fines reconstitution (MF) or hand destructuration and slurry (SD). The NCL and CSL of the MD specimens are above the lines determined for the unreinforced CDG prepared with the same method, at a vertical distance of about 0.03 (within an error margin of ± 0.01).

The effect of the fiber reinforcement on the size of the state boundary surface can be determined by normalizing the triaxial stress paths for volume, by using an equivalent pressure on a reference line in v-lnp' space (Figure 7). Figure 7a identifies the state boundary surface of the unreinforced CDG and Figure 7b the surface for the reinforced CDG. The CSL is taken here as the reference line, using the appropriate CSL corresponding to the reinforced CDG and unreinforced CDG, either MD/DD or SM/MF as relevant, to determine the equivalent pressure $p_{cs}' = \exp\left(\frac{\Gamma - v}{\lambda}\right)$, with the values of Γ and λ as determined in Table 2. The different values of M for the reinforced and unreinforced CDG explain the shift of the normalized critical state line (plotted as a point) upwards for the fiber-CDG. With the type of normalization applied, the stress paths for the reinforced CDG plot within the state boundary surface for the unreinforced CDG. Some hand destructured and slurried specimens (SD), both reinforced and unreinforced, only joined the iso-NCL at large stresses so for the triaxial compression tests at low confining stress the value of p'/p'_{cs} at the start of shearing can be as high as 3.0.

Further insight on the mechanics of the fiber-CDG mixture

Effect of overconsolidation

A series of drained tests was performed to investigate the effect of overconsolidation on the performance of the CDG reinforced with type-A fibers. Two over-consolidated (OC) specimens with an overconsolidation ratio OCR = 6 were sheared from p' = 50 and 100 kPa and one with an OCR of 3 was tested from p' = 200 kPa. The test results obtained from these specimens can be compared with the normally consolidated (NC) specimens sheared at p' = 50, 100 and 200 kPa already presented above. It was difficult to obtain the same void ratio for the NC specimens and their corresponding OC specimens, but a comparison can be made by taking account of the state of the specimens, summarized in the inset on Figure 8a, which shows the specimen initial states prior to shearing. Because of the large stresses required to reach the NCL, none of the “normally consolidated” specimens lie on it at the start of shearing, however, apart from specimen RA2MD50, they plot to the right of the CSL and therefore should display a contractive behavior upon shearing. All three overconsolidated specimens are on the “dry” side of critical (i.e. to the left of the CSL) and are expected to dilate upon shearing.

Figures 8a and 8b show the stress-strain and volumetric responses respectively, the overconsolidated specimens being represented by open symbols. It is obvious from Figure 8a that the overconsolidated specimens reach a lower deviatoric stress at failure than the normally consolidated specimens sheared at the same confining pressure, by 75% at the low confining stress of 50 kPa, the difference reducing to 8% at the higher confining stress of 200 kPa. They also display a more dilative behavior (Fig. 8b), which can be predicted from their initial state on the “dry” side of critical. Two specimens starting from comparable states slightly to the left of the CSL, RA2MD50 (OCR = 1) and RA1SD200 (OCR = 3), show the same amount of volumetric deformation. Only specimen RA1MD200 displays unexpected dilative behavior considering the high initial void ratio, which may be attributed to some localization within the specimen. It was also highlighted above for behaving unusually and reaching a lower strength than expected (Fig. 3a). The OC specimens have a high initial stiffness, mobilizing their strength rapidly from low strains. The stress dilatancy shown in Figure 8c emphasizes that rapid gain in strength in the overconsolidated specimens with almost no volumetric deformation up to the peak stress ratio while the normally consolidated specimens follow a path typical of frictional materials, compressing to the maximum value of q/p'. The value of q/p' at critical state is much less for the OC specimens, with M = 1.75, than for the NC specimens which reached M = 2.25. It is interesting that against preconceptions that fibers should be mobilizing tensile resistance when shear strains develop, when comparing with the OC specimens, which tend to dilate, the NC specimens (which contract upon shearing) reach higher strengths. It therefore seems that tensile strains are not the only requirement for fibers to mobilize strength, and that their complex orientation within the specimen combined with the continuous particle rearrangement during shearing contribute with a non-negligible part to the resistance. Unfortunately, unless experimental micromechanical studies of the fiber-soil interaction mechanism are made it is difficult to be certain about this.

Fiber-soil grains interaction

The CDG, which contains about 20% fines, behaves differently when the sample preparation method involves a large amount of water (e.g. by making a slurry), which may separate the fines attached to the coarse particles by light cementation than it does when prepared dry or moist-tamped. The main effect is a shift in the locations of the NCL and CSL in the v-lnp' plane (e.g. Fig. 2, 6). It has been shown that unlike for the unreinforced CDG, adding fibers seems to lead to a more homogenous response with unique critical state and normal compression lines, independently of the fines free to move in the soil matrix. In the q-p' plane, the well-graded nature of the soil also seems to make the fibers effective even at very large stresses (Figure 4), unlike what is usually found or hypothesized for fiber-soil mixtures (e.g. Maher and Gray, 1990; Silva dos Santos et al., 2010). The contribution of clay particles to the bonding and friction between soil and fibers was shown by Tang et al. (2007) who combined single fiber pull out tests in small samples of clayey silt with scanning electron microscopy. Tang et al. (2016) also showed that coarse grains can increase the roughness of the fibers by plowing and thus their interlocking strength. Monitoring the particle breakage in the specimens may provide further insight into the fiber-soil interaction: Silva dos Santos et al. (2010) showed how a significant amount of fibers break during isotropic compression to high stresses, some of them possibly by nipping, and further are broken during shearing. The specimens were sieved before and after the drained high pressure triaxial tests (Figure 9). As was found by Silva dos Santos et al. (2010) for uniform sand, the unreinforced specimens suffered more breakage than the reinforced ones. The moist-tamped specimens were the most affected. It is expected that, in specimens where fines were released during the sample preparation, the higher number of contacts between grains would lead to less breakage, but little difference is seen between the different methods of preparation, suggesting that the fibers might have hindered the force transmitting contacts between particles in all specimens. Upon examination of the fibers after test, it was found that some fibers were twisted, some were elongated and a significant but not extensive amount was broken, which reinforces the finding that fibers added to well graded weathered soil have a potential to mobilize strength even at large confining stress.

Conclusions

This study showed that adding discrete fibers to a well graded completely decomposed granite can improve its performance. Similarly to what was found in previous research for uniform quartzitic sands, a low fiber content is enough to gain significant additional strength in the reinforced soil, with values of stress ratio at critical state 20 to 40% greater than that of their unreinforced counterparts. The normal compression line and critical state line of the reinforced soil are parallel and above those of the unreinforced soil. The fibers also seem to reduce the amount of grain breakage during compression. Two additional fundamental points that should contribute to the database on fiber-soil composites have been highlighted:

- Fibers were found to contribute to the strength of the soil despite the compressive nature of the host soil, thus showing that tensile strains are not the only requirement for fibers to mobilize their strength, but that the complex combination of fiber orientation, fiber stiffness and continuous particle rearrangement also contribute to the resistance.
- In completely decomposed granite, which contains a non-negligible amount of fines, the method of sample preparation, in particular adding a large amount of water at the stage of material or sample preparation, affects the fabric and the overall behavior, such

as the location of the NCL and CSL. The reinforced CDG however was found to have a unique normal compression line and a unique critical state line independently of the method of sample preparation, the fibers having a homogenizing effect on the mixture.

Acknowledgements

This research was made possible thanks to the financial support provided by the Hong Kong Research Grant Council (grant GRF No.710211). The authors are also indebted to Professor Nilo Consoli from the University Federal of Rio Grande do Sul for providing the fibers.

References

Ang, E.C., and Loehr, J.E. (2003). “Specimen Size Effects for Fiber-Reinforced Silty Clay in Unconfined Compression”. *Geotechnical Testing Journal*, 26(2), 1-10.

Ajayi, O., Le Pen, L., Zervos, A., and Powrie, W. (2016). “A behavioral framework for fibre reinforced gravel.” *Géotechnique,* (In Press), DOI:10.1680/jgeot.16.P.023.

Altuhafi F., Baudet B.A., and Sammonds P. (2010). “The mechanics of subglacial sediment: an example of new “transitional behavior”." *Canadian Geotechnical Journal*, 47 (7), 775-790.

Consoli, N. C., Casagrande, M. D. T., Thomé, A. and Prietto, P. D. M. (2003). “Plate load test on fiber-reinforced soil.” *J. Geotech.Geoenviron. Eng.*, 129(10), 951–955.

Consoli, N.C., Casagrande, M.D.T., and Coop, M.R. (2005). “Effect of fiber reinforcement on the isotropic compression behavior of a sand.” *J. Geotech. Geoenviron. Eng.*, 131(11), 1434-1436.

Coop, M.R., and Lee, I.K. (1993). “The behavior of granular soils at elevated stresses.” In: *Predictive soil mechanics*, Proc. of the C. P. Wroth Memorial Symposium (Houlsby and Schofield eds.), pp. 186–198. London, UK: Thomas Telford.

Coop, M.R., Sorensen, K.K., Bodas Freitas, T., and Georgoutsos, G. (2004). “Particle breakage during shearing of a carbonate sand.” *Géotechnique,* 54(3), 157–163.

Diambra, A., Ibraim, E., Russell, A. R., and Muir Wood, D. (2013). “Fibre reinforced sands: from experiments to modelling and beyond”. *International Journal for Numerical and Analytical Methods in Geomechanics*, 37(15), 2427-2455

Diambra, A., and Ibraim, E. (2015). “Fiber-reinforced sand: interaction at the fiber and grain scale.” *Géotechnique*, 65(4), 296-308.

Ekinci, A., and Ferreira, P.M.V. (2013). “Effects of fibre inclusion on stress strain behavior of a compacted over-consolidated clay from Lambeth group.” In: Proc. Int. Conf. Ground Improv. Ground Control (Indraratna et al. eds.), ICGI Wollongong 2012, pp. 912-917. Singapore: Research Publishing Services.

Ferreira, P.M.V., and Bica, A.V.D. (2006). “Problems on the identification of structure in a soil with a transitional behavior.” *Géotechnique*, 56(7), 445–454.

GEO Publication No.1/2011 www.cedd.gov.hk/eng/publicatios/geo/doc/ep1_2011.pdf

Ghazavi, M., and Roustaie, M. (2010). “The influence of freeze-thaw cycles on the unconfined compressive strength of fiber-reinforced clay.” *Cold Reg. Sci. Technol.*, 6,125–131.

Gray, D.H., and Al-Refeai, T. (1986). “Behavior of fabric versus fiber reinforced sand.” *J. Geotech. Eng.,* 112(8), 804-826.

Gray, D.H., and Ohashi, H. (1983). “Mechanics of fiber-reinforcement in sand.” *J. Geotech. Eng.,* 109(3), 335-353.

Gregory, G. (2011). “Sustainability and the fiber-reinforced soil repair of a roadway embankment.” *Geosynthetics Magazine*, Bouquet 08, August 2011.

Hall, S.A., Bornert, M., Desrues, J., Pannier, Y., Lenoir, N., Viggiani, G., and Bésuelle, P. (2010). ”Discrete and continuum analysis of localised deformation in sand using X-ray µCT and volumetric digital image correlation.” *Géotechnique*, 60(5), 315-322.

Head, K.H. (1980). *Manual of soil laboratory testing*, 3 vols. London, Plymouth, UK: Pentek.

Ladd, R.S. (1978). “Preparing test specimens using under-compaction.” *Geotech. Testing J.*, 1(1): 16-23.

Lee, I.K., and Coop, M.R. (1995). “The intrinsic behavior of a decomposed granite soil.” *Géotechnique*, 45(1), 117–130.

Madhusudhan, B.N., and Baudet, B.A (2014). “Influence of reconstitution method on complete decomposed granite soil.” *Géotechnique,* 64(7), 540-550.

Maher, M.H., and Gray, D.H. (1990). “Static response of sands reinforced with randomly distributed fibers.” *J. Geotech. Eng.*, 116(11), 1661-1677.

Maher, M.H., and Ho, Y.C. (1994). “Mechanical properties of kaolinite/fiber soil composite.” *J. Geotech. Eng*., 120(8), 1381-1393.

Michalowski, R.L., and Cermak, J. (2003). “Triaxial compression of sand reinforced with fibers.” *J. Geotech. Geoenviron. Eng.*, 129(2), 125-136.

Muir Wood, D. (2006). “Geomaterials with changing grading: a route towards modelling.” *Proc. Int. Symp. Geomech. Geotech. Particulate Media, Ube, Yamaguchi, Japan: Geomechanics and Geotechnics of Particulate Media* (eds. M. Hyodo, H. Murata and Y. Nakata), pp. 313–325. London, UK: Taylor and Francis Group.

Salvagni Heineck, K., Coop, M.R., and Consoli, N.C. (2005). “Effect of microreinforcement of soils from very small to large shear strains.” *J. Geotech. Geoenviron. Eng.*, 131(8), 1024-1033.

Santucci, F., Silvestri, F., and Vinale, F. (1998). “The influence of compaction on the mechanical behavior of a silty sand.” *Soils and Foundations,* 38(4), 41-56.

Silva dos Santos, A.P., Consoli, N.C., and Baudet, B.A. (2010). “The mechanics of fiber-reinforced sand.” *Géotechnique*, 60(10), 791-799.

Tang, C.S., Shi, B., Gao, W., Chen, F., and Cai, Y. (2007). “Strength and mechanical behavior of short polypropylene fiber reinforced and cement stabilized clayey soil” *Geotextiles and Geomembranes* 25, 194-202.

Tang, C.S., Shi, B., and Zhao, L.Z. (2010). “Interfacial shear strength of fiber reinforced soil.” *Geotextiles and Geomembranes* 28, 54-62.

Viana da Fonseca, A., Carvalho, J., Ferreira, C., Santos, J.A., Almeida, F., Pereira, E., Feliciano, J., Grade, J., and Oliveira, A. (2006). “Characterization of a profile of residual soil from granite combining geological, geophysical and mechanical testing techniques.” *Geotech. Geol. Eng.,* 24, 1307-1348.

Yan, W.M, and Li, X.S. (2012). “Mechanical response of medium-fine-grained decomposed granite in Hong Kong.” *Eng. Geol.*, 129-130, 1-8.

Zornberg, J.G. (2005). “Advances in Reinforced Soil Technology.” *Proc. Int. Symp. Geosynth. Applications Ground Reinforcement and Improvement*, July 6-7, Busan, South Korea, pp. 155-196.

Table 1 - Summary of the triaxial tests performed on reinforced and unreinforced CDG.

Test	w_0 (%)	v_0	v_c	Specific volume precision	p_c' (kPa)	OCR	Method	γ_d (kN/m³)	Test type
	Type A: fiber length = 24 mm, fiber content = 0.3%								
RA2MD50	11.4	1.52	1.50	0.012	49	1	MD	17.06	CID
RA1MD100	11.0	1.66	1.51	0.011	100	1	MD	15.62	CID
RA2MD100	10.6	1.67	1.40	0.042	99	6	MD	16.41	CID
RA1MD200	11.3	1.54	1.46	0.020	203	1	MD	17.95	CID
RA1MF500	11.2	1.59	1.40	0.025	499	1	MF	16.11	CID
RA1MD K_0	11.2	1.57	1.38	0.025	635	-	MD	16.22	CK_0D
RAMD HP	11.0	1.53	1.18	0.02	20000	1	MD	16.95	HP CID
RA1SD50	19.8	1.52	1.42	0.018	48	6	SD	17.05	CID
RA1SD200	20.1	1.67	1.40	0.041	210	3	SD	15.97	CID
RA1SD340	20.0	1.59	1.45	0.032	341	1	SD	17.65	CID
RA1SD500	20.4	1.64	1.42	0.024	500	1	SD	16.95	CID
RA1SD750	20.3	1.65	1.36	0.038	749	1	SD	16.05	CID stress Path
RA1SD1000	20.4	1.54	1.38	0.005	984	1	SD	17.06	CID
RA2SD1000	20.6	1.60	1.37	0.025	1000	1	SD	17.45	CIU
RA1SD1200	20.5	1.55	1.35	0.010	1200	1	SD	17.28	CID
RA1SD K_0	18.4	1.53	1.34	0.015	1065	-	SD	16.78	CK_0U
RA SD HP	20.6	1.53	1.19	0.02	20015	1	SD	17.44	HP CID
	Type C: fiber length = 50 mm, fiber content = 0.3%								
RC1SD100	20.4	1.56	1.46	0.021	98	1	SD	16.65	CID
RC1SD1350	20.3	1.62	1.37	0.025	1300	1	SD	16.23	CID

RC1SD K_0	20.5	1.52	1.35	0.007	909	-	SD	17.21	CK_0U
	Type D: fiber length = 50 mm, fiber content = 0.1%								
RD1MD100	11.1	1.64	1.52	0.030	97	1	MD	15.85	CID
RD1MD500	11.2	1.62	1.43	0.010	495	1	MD	15.51	CID
	Unreinforced CDG (data from Madhusudhan and Baudet, 2014)								
URDD50	0.1	1.51	1.47	0.012	45	1	DD	17.06	CID
URSD100	20.3	1.58	1.46	0.021	112	1	SD	16.04	CID
URDD500	0.1	1.50	1.34	0.007	494	1	DD	17.87	CID
URMF K_0	11.2	1.64	1.41	0.021	923	-	MF	17.41	CK_0D
URDD K_0	0.1	1.50	1.29	0.012	923	-	DD	15.85	CK_0D
URMD HP	11.0	1.44	1.10	0.04	30027	1	MD	18.03	HP CID
URMF HP	11.1	1.52	1.17	0.05	30086	1	MF	17.77	HP CID

w_0 initial water content; v_0 initial specific volume; v_c specific volume after consolidation (before shearing); p_c' mean effective stress before shearing; γ_d dry density

Test type: CID: isotropically consolidated drained test; CIU: isotropically consolidated undrained test; CK_0D: K_0-consolidated drained test; CK_0U: K_0-consolidated undrained test; HP: High Pressure tests

Preparation method: DD: Dry deposition and hand Destructuration; MD: Moist tamping and hand Destructuration; SD: Slurry and hand Destructuration; MF: Moist tamping and Fines reconstitution

Table 2 Summary of the normal compression and critical state parameters for the reinforced and unreinforced CDG

	Sample preparation	Isotropic NCL		CSL		
		λ	N	λ	Γ	M
Unreinforced CDG	D/M	0.061	1.73	0.061	1.69	1.57
	S/F	0.061	1.82	0.061	1.75	1.57
Reinforced CDG	All preparations	0.061	1.81	0.061	1.75	1.90

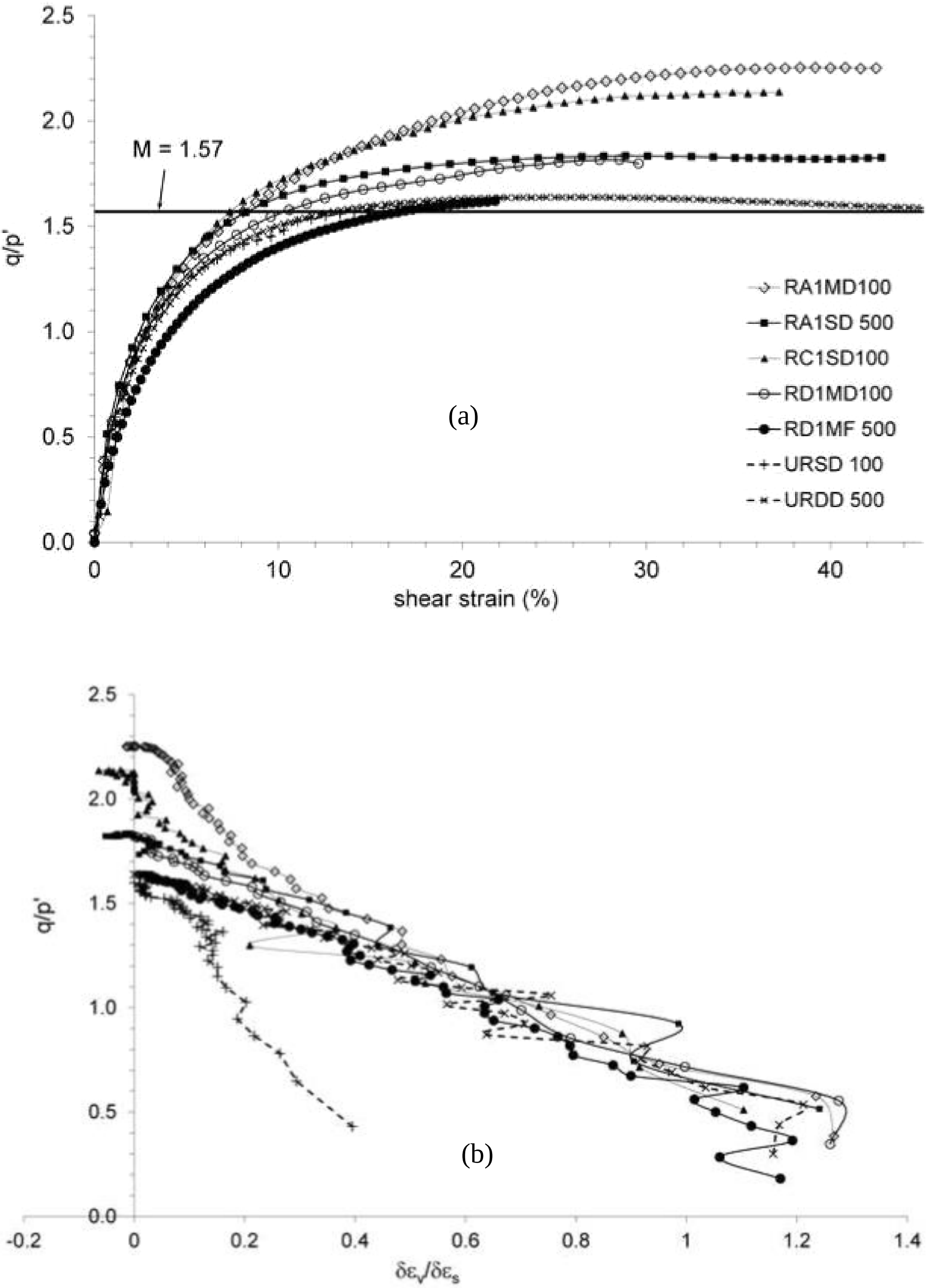

Figure 1- Determination of the optimum fiber-soil mixture form tests on CDG prepared with different fiber types and dosages (a) stress-strain response (b) stress dilatancy.

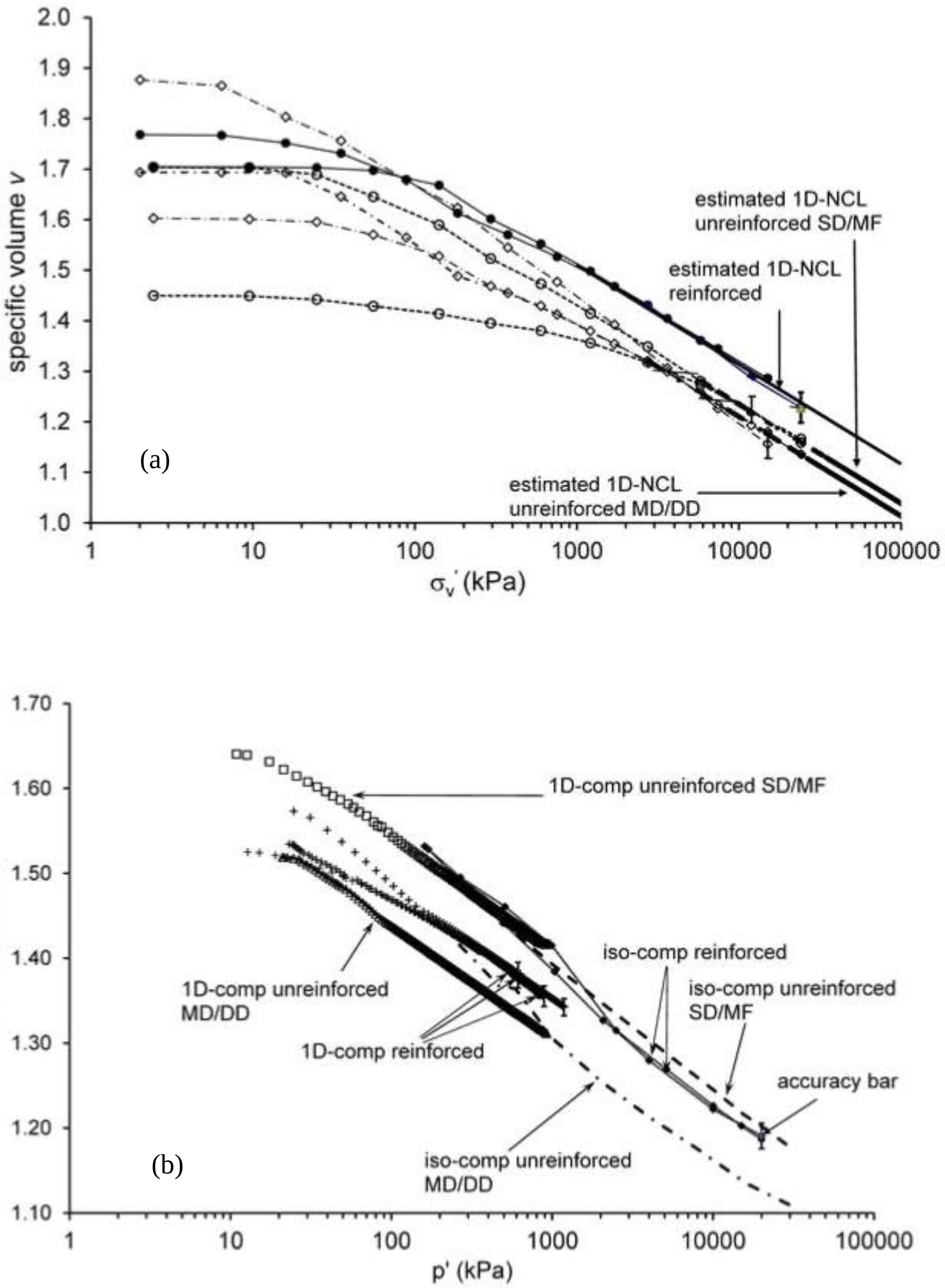

Figure 2 - (a) Oedometer and (b) triaxial one-dimensional and isotropic compression curves of reinforced and unreinforced CDG prepared with different methods. Unreinforced soil test data from Madhusudhan and Baudet (2014).

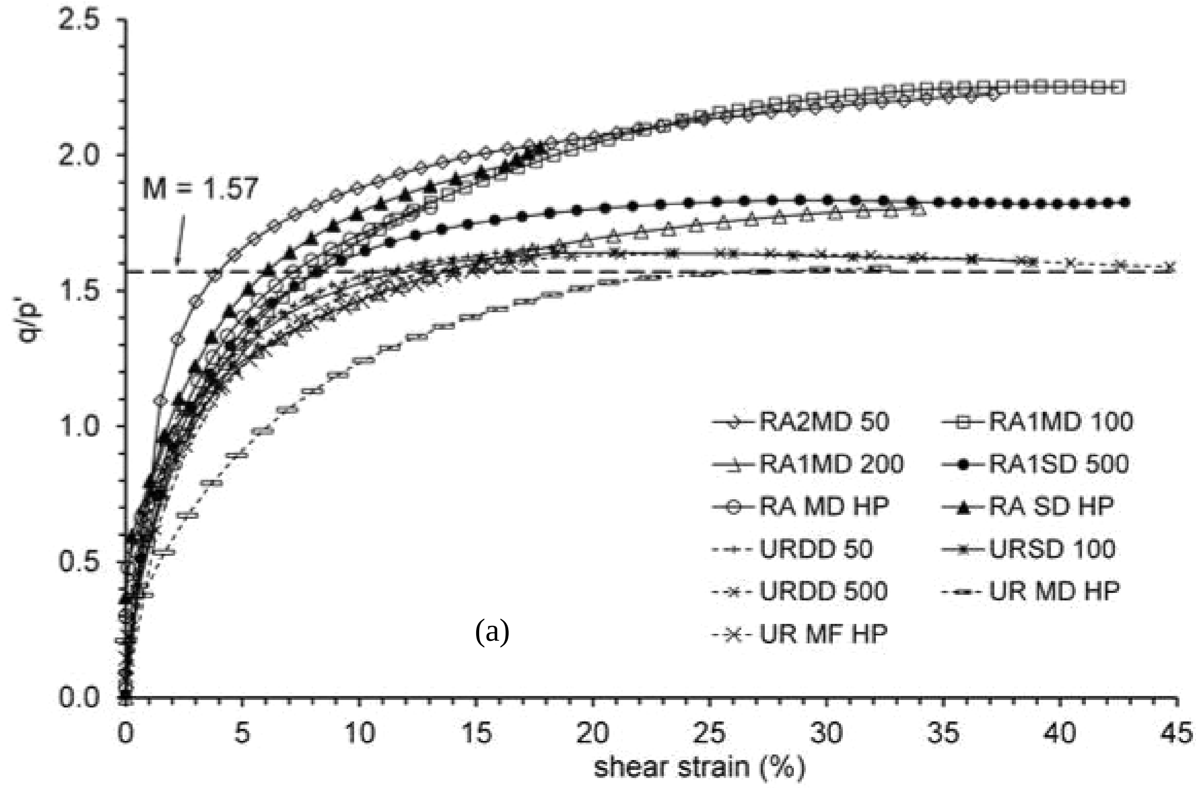

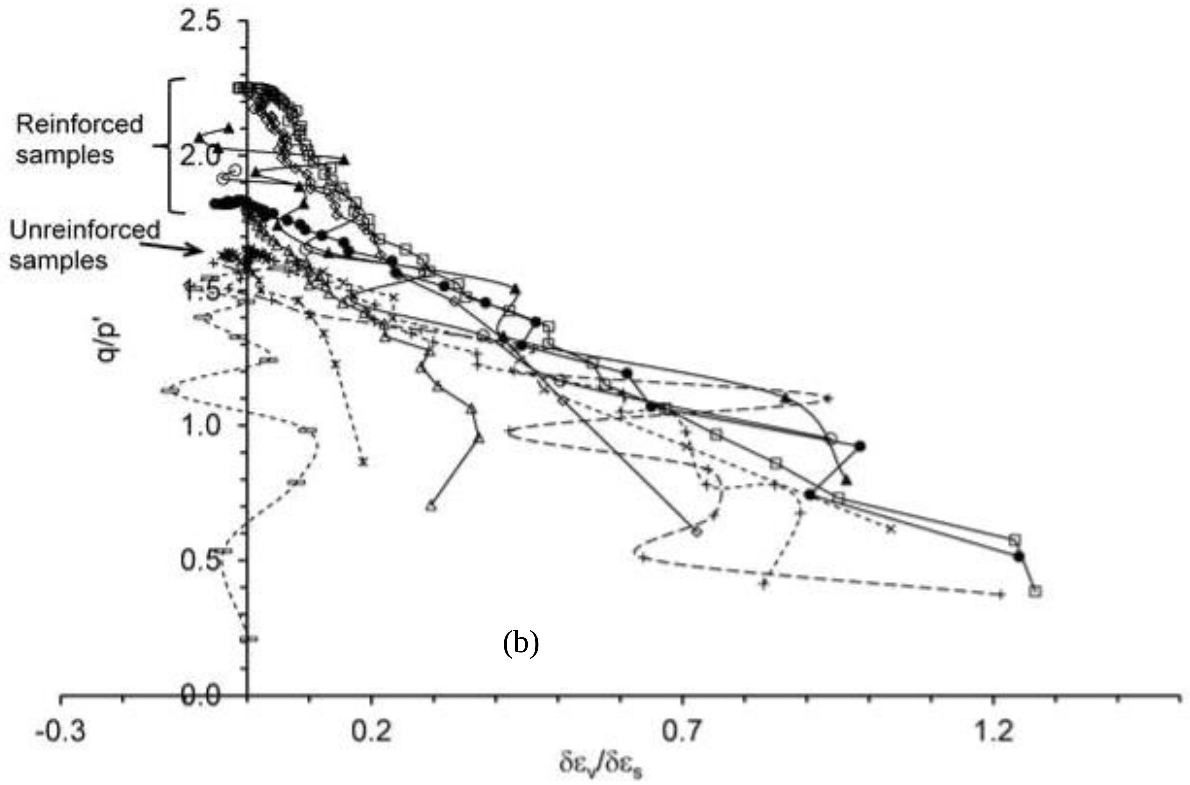

Figure 3 - Effect of material and sample preparation on the shearing behavior of CDG reinforced with type-A fibers (a) stress-strain response (b) stress dilatancy

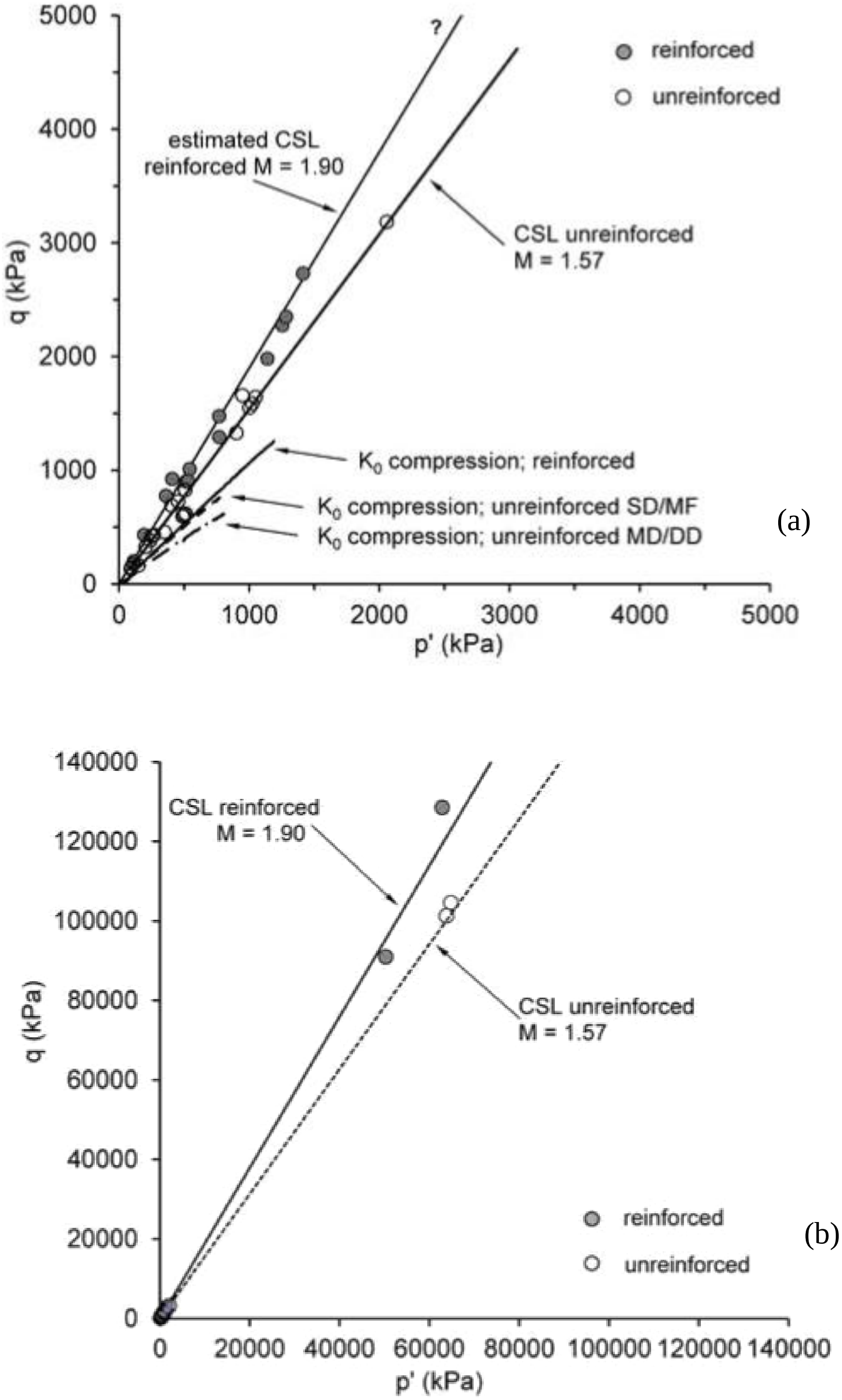

Figure 4 - Determination of the critical state line in (a) low to medium stress space (b) including the high pressure test data. The one-dimensional compression paths are also shown.

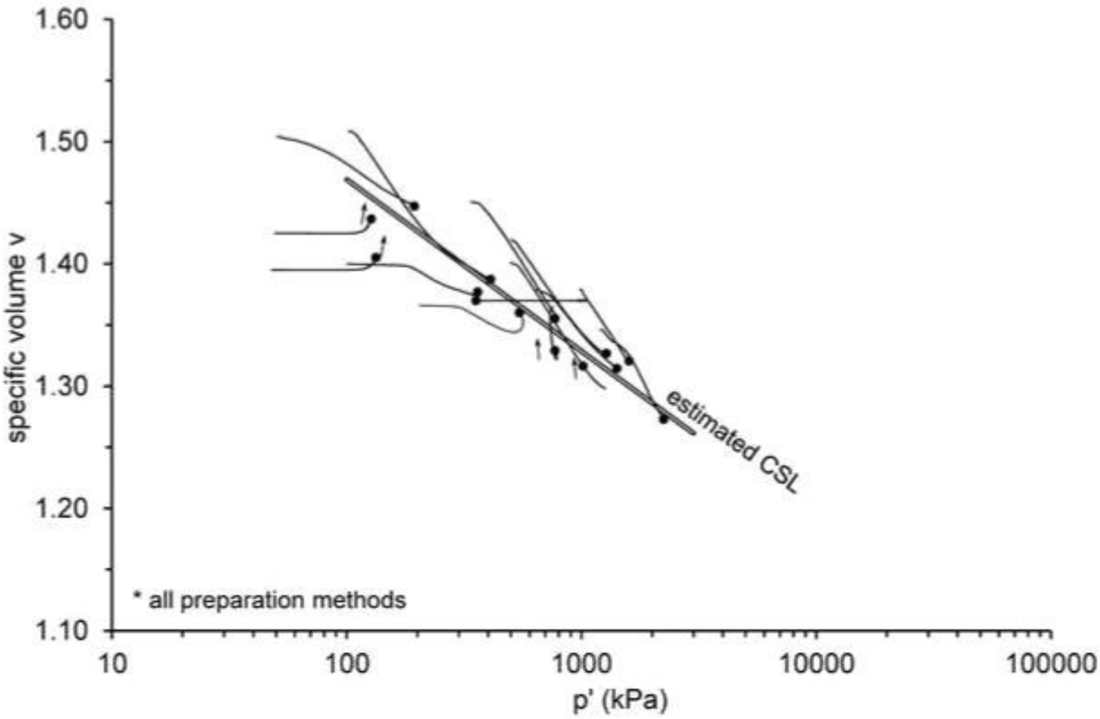

Figure 5 - Determination of the CSL of CDG reinforced with type-A fibers in state space

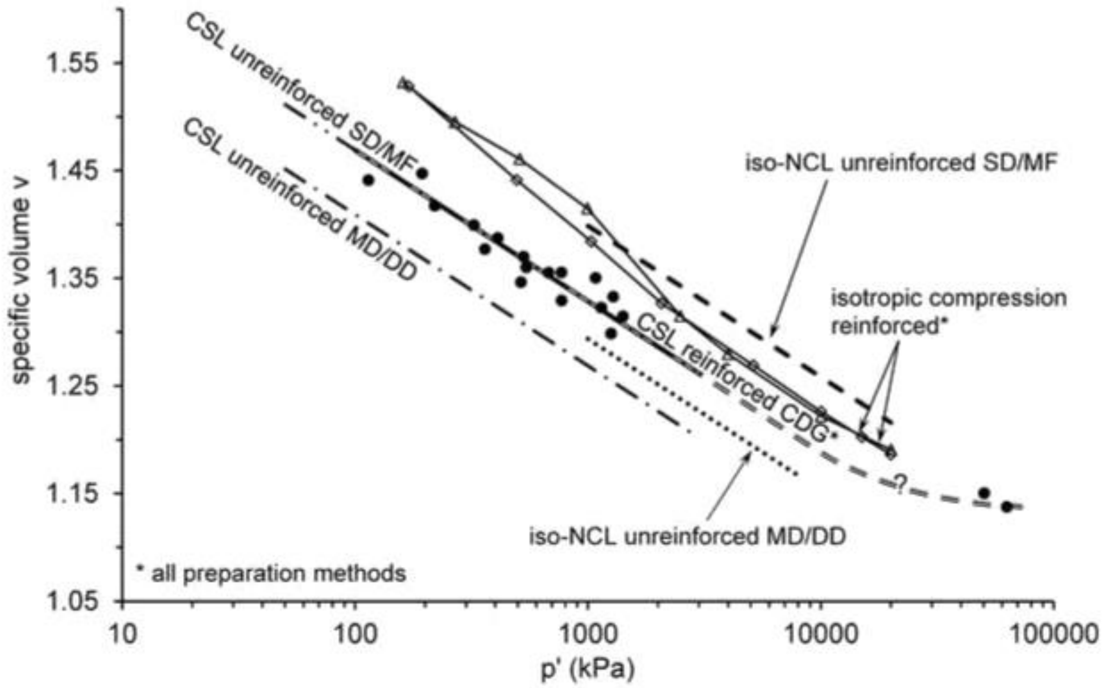

Figure 6 - Summary of normal compression and critical state lines obtained for the unreinforced CDG and CDG reinforced with type-A fibers.

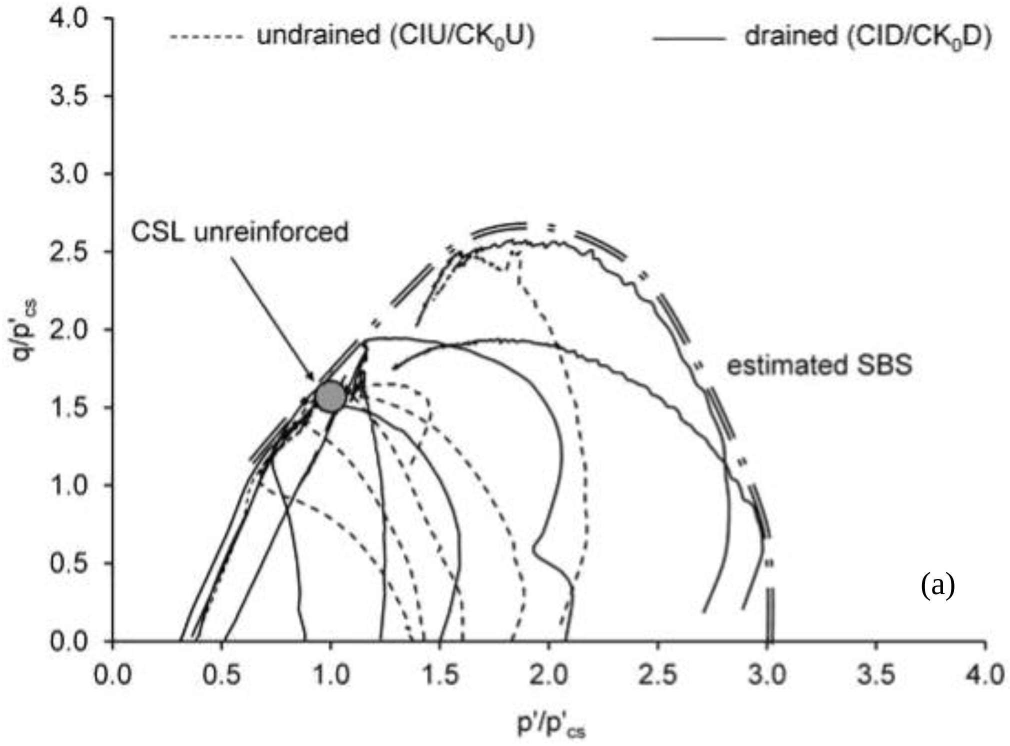

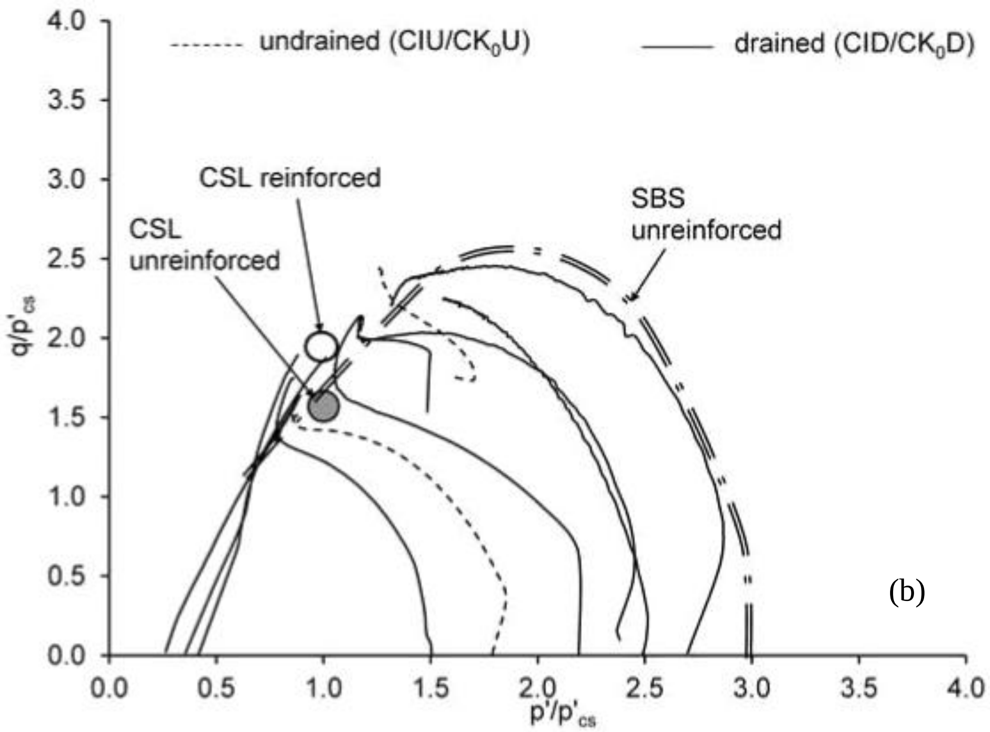

Figure 7 - State boundary surface of the (a) unreinforced CDG and (b) CDG reinforced with type-A fibers. The mean effective stresses have been normalized with respect to an equivalent pressure on the corresponding CSL.

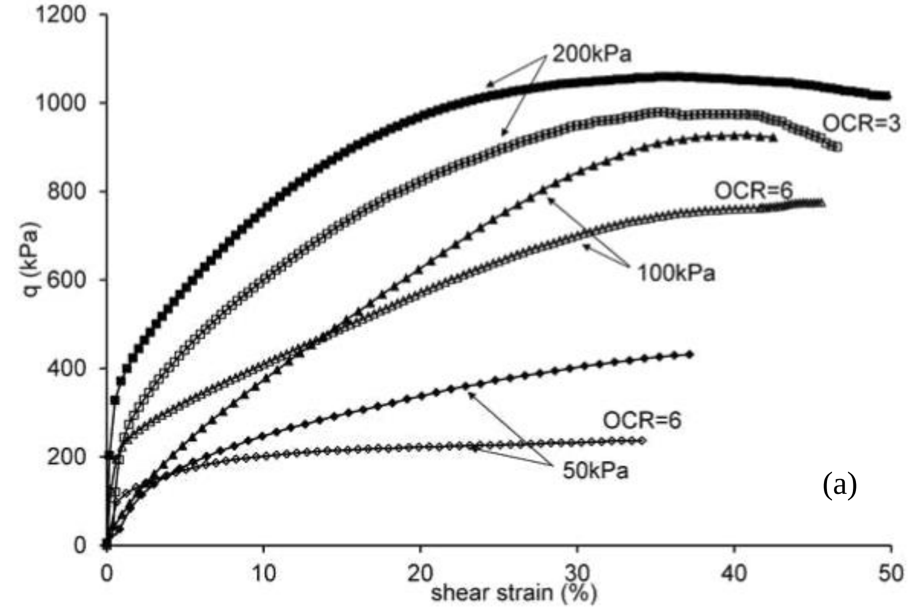

1200
1000
800
600
400
200
0
q (kPa)
200kPa
OCR=3
OCR=6
100kPa
OCR=6
50kPa
(a)
0
10
20
30
40
50
shear strain (%)

1

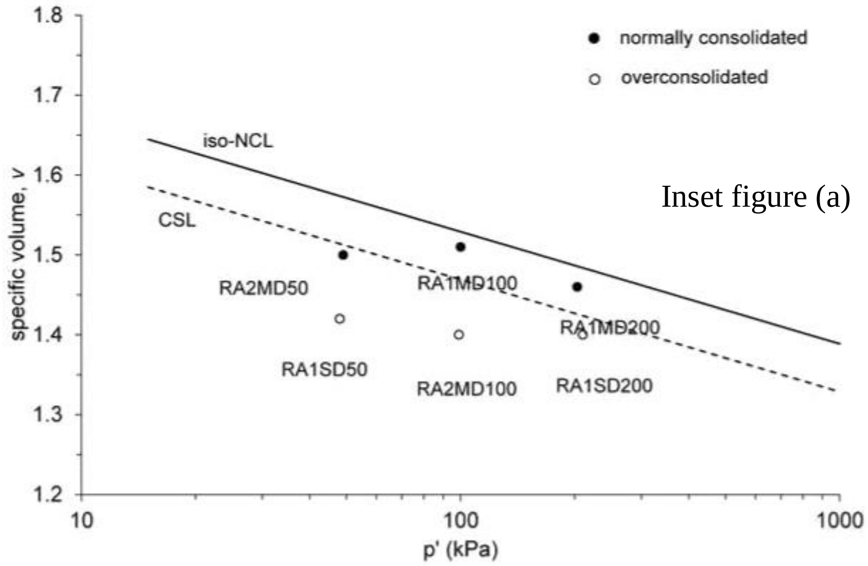

normally consolidated
overconsolidated
iso-NCL
CSL
Inset figure (a)
specific volume, v
RA2MD50
RA1MD100
RA1MD200
RA1SD50
RA2MD100
RA1SD200
1.8
1.7
1.6
1.5
1.4
1.3
1.2
10
100
1000
p' (kPa)

2

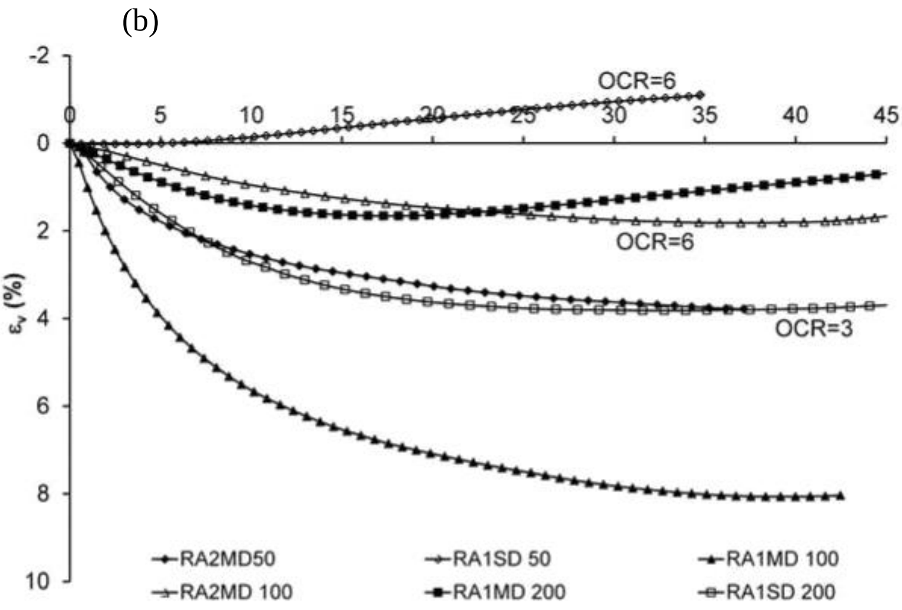

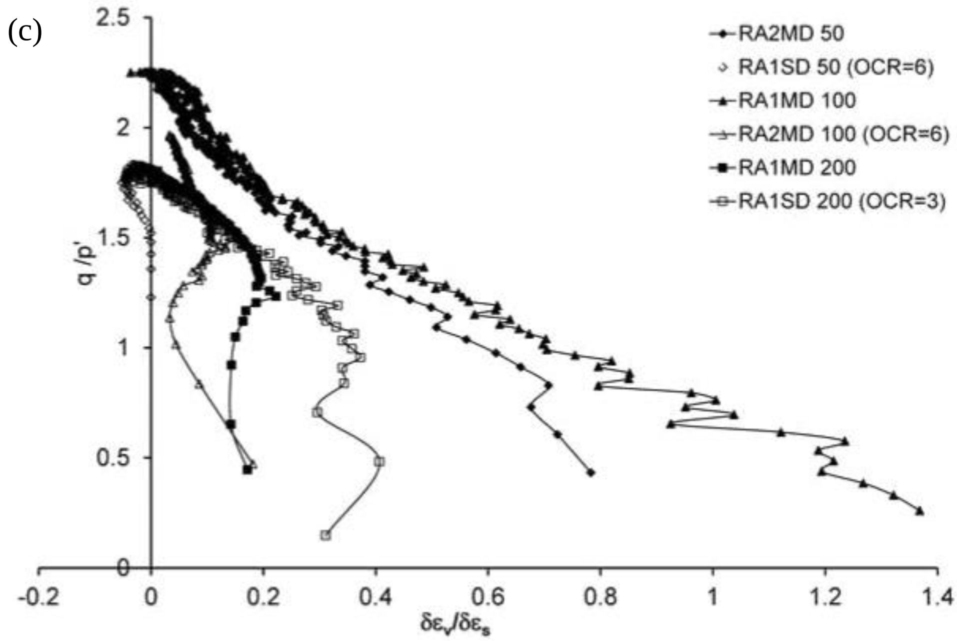

Figure 8 - Effect of overconsolidation on the (a) stress-strain response (inset critical state points on v-logp' space) (b) volumetric strain response and c) stress dilatancy of the type-A reinforced CDG.

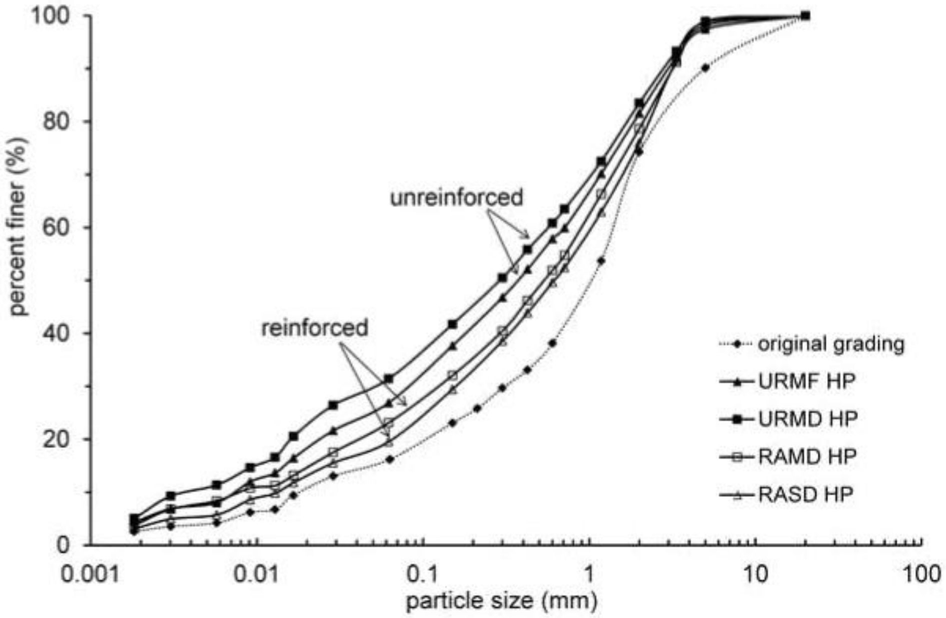

Figure 9 - Effect of fibers on the amount of particle breakage during drained compression to high pressure.